BASIC RESEARCH PAPER

Autophagy 9:10, 1579–1590; October 2013; © 2013 Landes Bioscience

Enhanced autophagy blocks angiogenesis via degradation of gastrin-releasing peptide in neuroblastoma cells

Kwang Woon Kim,[1] Pritha Paul,[1,2] Jingbo Qiao,[1] Sora Lee,[1] and Dai H Chung[1,2,*]

[1]Department of Pediatric Surgery; Vanderbilt University Medical Center; Nashville, TN USA; [2]Department of Cancer Biology; Vanderbilt University Medical Center; Nashville, TN USA

Keywords: autophagy, angiogenesis, GRP, neuroblastoma, endothelial cells, rapamycin

Abbreviations: ACTB, actin beta; ATG, autophagy-related; BAFA1, bafilomycin A_1; GRP, gastrin-releasing peptide; GRPR, gastrin-releasing peptide receptor; GFP-LC3, green fluorescent protein-microtubule-associated protein 1 light chain 3; NB, neuroblastoma; HUVECs, human umbilical vein endothelial cells; MTOR, mechanistic target of rapamycin; RPS6, ribosomal protein S6; SQSTM1/p62, sequestosome 1; v-ATPase, vacuolar-type H^+-ATPase

Neuroblastoma is characterized by florid vascularization leading to rapid tumor dissemination to distant organs; angiogenesis contributes to tumor progression and poor clinical outcomes. We have previously demonstrated an increased expression of gastrin-releasing peptide (GRP) and its receptor, GRPR, in neuroblastoma and that GRP activates the PI3K-AKT pathway as a proangiogenic factor during tumor progression. Interestingly, AKT activation phosphorylates MTOR, a critical negative regulator of autophagy, a cellular process involved in the degradation of key proteins. We hypothesize that inhibition of GRPR enhances autophagy-mediated degradation of GRP and subsequent inhibition of angiogenesis in neuroblastoma. Here, we demonstrated a novel phenomenon where targeting GRPR using shRNA or a specific antagonist, RC-3095, decreased GRP secretion by neuroblastoma cells and tubule formation by endothelial cells in vitro. Furthermore, sh*GRPR* or RC-3095 treatment enhanced expression of proautophagic proteins in human neuroblastoma cell lines, BE(2)-C, and BE(2)-M17. Interestingly, rapamycin, an inhibitor of MTOR, enhanced the expression of the autophagosomal marker LC3-II and GRP was localized within LC3-II-marked autophagosomes in vitro as well as in vivo, indicating autophagy-mediated degradation of GRP. Moreover, overexpression of ATG5 or BECN1 attenuated GRP secretion and tubule formation, whereas opposite effects were observed with siRNA silencing of *ATG5* and *BECN1*. Our data supported the role of autophagy in the degradation of GRP and subsequent inhibition of angiogenesis. Therefore, activation of autophagy may lead to novel antivascular therapeutic strategies in the treatment of highly vascular neuroblastomas.

Introduction

Neuroblastoma (NB), a tumor derived from neural crest precursors, is the most common extracranial solid malignancy in infants and children, accounting for approximately 15% of all pediatric cancer-related deaths in the US.[1] NB is characterized by intense angiogenesis, which in turn contributes to aggressive tumor behavior by stimulating tumor growth, invasion and metastasis, and ultimately poor patient outcomes.[2] Angiogenesis, or the ability of malignant tumors to establish their own blood supply, depends mainly on the release of specific growth factors by cancer cells and/or nearby cells.[3] Recently, we have demonstrated the critical role of gastrin-releasing peptide (GRP), a gut neuropeptide, and its receptor, GRPR, in neuroblastoma initiation and progression. Higher expression of GRP or GRPR correlates with aggressive clinical behavior of neuroblastomas.[4] Interestingly, bombesin, the amphibian equivalent of GRP, stimulated expression of angiogenic markers and neuroblastoma growth in vivo.[5]

Silencing *GRPR* downregulates the AKT-RPS6 signaling axis, which is critical in stimulating neuroblastoma cell proliferation, and anchorage-independent growth along with angiogenesis in vitro.[6] Activated AKT phosphorylates MTOR via phosphorylation of tuberous sclerosis complex (TSC2), a direct target of AKT.[7] MTOR is a critical negative regulator of autophagy.[8] However, whether silencing *GRPR* regulates MTOR signaling and in turn autophagy in neuroblastoma cells has not been examined. Autophagy is a highly conserved and regulated catabolic phenomenon involved in the degradation of long-lived proteins and recycling cellular components such as

*Correspondence to: Dai H Chung; Email: dai.chung@vanderbilt.edu
Submitted: 10/18/2012; Revised: 07/29/2013; Accepted: 07/31/2013
http://dx.doi.org/10.4161/auto.25987

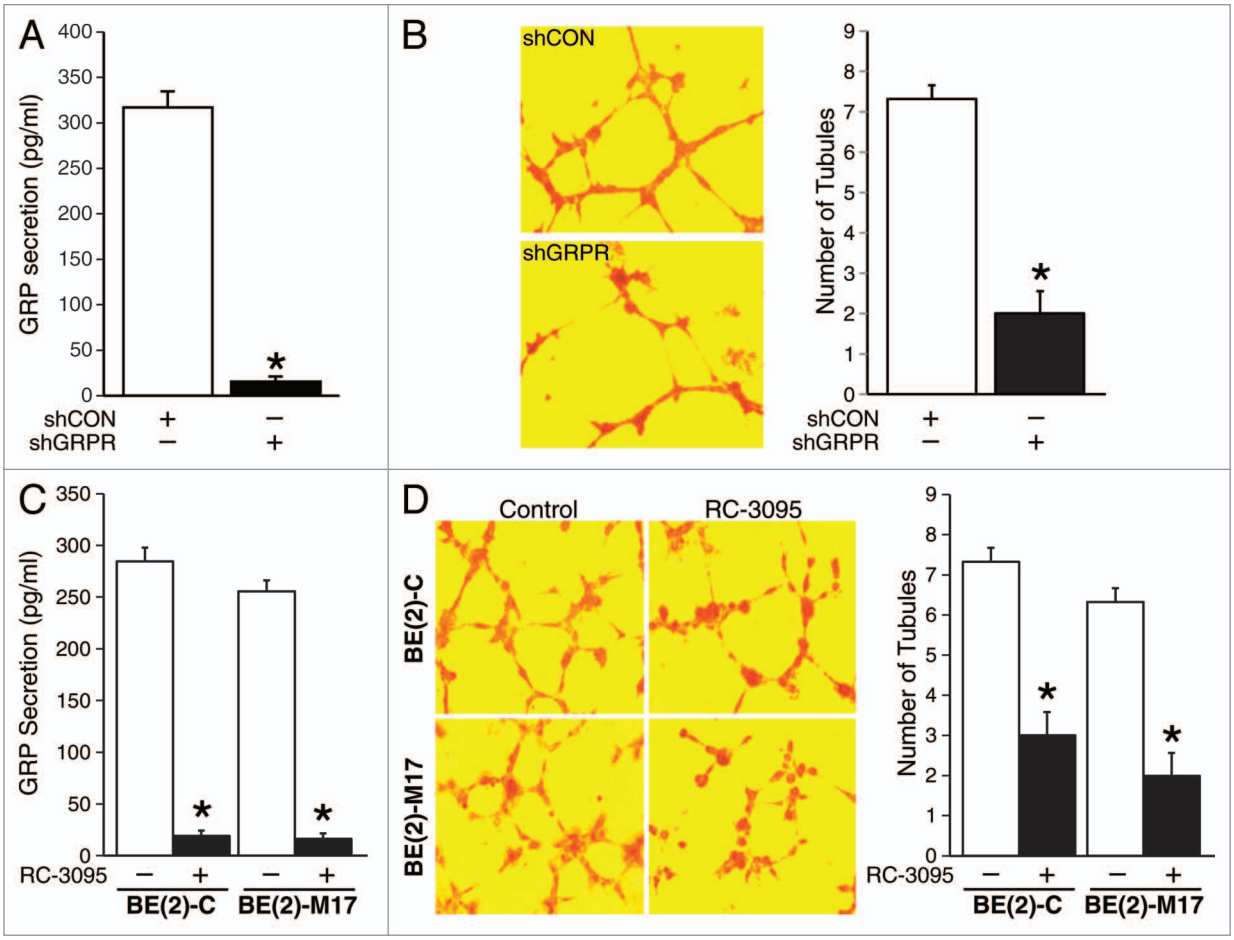

Figure 1. Inhibition of GRPR decreased GRP secretion in human neuroblastoma cells. (**A**) BE(2)-C cells stably-transfected with either shCON or sh*GRPR* were plated in serum-free media for 48 h and analyzed for GRP secretion by ELISA. (**B**) HUVECs were plated on 24-well plates coated with Matrigel and incubated with BE(2)-C cell culture media from either shCON or sh*GRPR*. After 6 h, cells were fixed and stained with H&E. Tubules were examined by microscopy and average number of tubules was counted from three separate fields of view. (**C**) BE(2)-C and BE(2)-M17 cells were plated in serum-free media and treated with DMSO or RC-3095 (1 μM) for 48 h. ELISA was used to analyze GRP secretion. (**D**) HUVECs were plated on 24-well plates coated with Matrigel and incubated with cell culture media from BE(2)-C or BE(2)-M17 cells treated with DMSO or RC-3095. Similar to (**B**), tubules were examined by microscopy. Values shown are mean ± SEM of three separate experiments (*$P < 0.05$ vs. shCON or without RC-3095).

mitochondria. It is characterized by the formation of cytoplasmic double-membrane vacuoles, named autophagosomes, which fuse with lysosomes.[9,10] This process has recently been identified as a physiological response to hypoxia-induced-angiogenesis and regression of hyaloid vessels.[11,12] Autophagy may potentially regulate angiogenesis by the lysosome-dependent degradation of hypoxia-inducible factor HIF1A/HIF-1α, a proangiogenic factor.[13] GRP undergoes degradation by a lysosomal or a phosphoramidon-sensitive pathway.[14] However, the exact role of autophagy-mediated pathway by which clearance of GRP may occur in neuroblastoma cells has not been explored.

Here we are reporting, for the first time, that targeting GRPR using shRNA or RC-3095 decreased GRP and increased expression of proautophagic proteins. We showed that enhanced autophagy increased the clearance of GRP in human neuroblastoma cells by an autophagy-mediated pathway. Our data indicated that autophagy-mediated decrease in GRP secretion decreases tubule formation by vascular endothelial cells in vitro and vascular density in vivo. Moreover, genetic modulation of the autophagic machinery confirmed the autophagy-mediated decrease in GRP secretion and subsequent inhibition of angiogenesis in vitro. Our findings suggest that autophagy can be used as a novel therapeutic strategy during neuroblastoma progression by targeting multiple hallmarks of cancer.

Results

Targeting GRPR inhibited angiogenesis by decreasing GRP secretion

GRP binds to GRPR to regulate angiogenesis during neuroblastoma progression.[5] Here, we wanted to determine whether silencing *GRPR* inhibits endogenous GRP-mediated angiogenesis using a previously established stable knockdown system in human neuroblastoma cell line, BE(2)-C.[6] To confirm this, we first assessed GRP secretion using *GRPR*-silenced

cells (sh*GRPR*) or controls (shCON). Using an ELISA-based detection kit specific for GRP, we found that GRP secretion by sh*GRPR* cells was significantly less in comparison to shCON (**Fig. 1A**). To determine whether this decrease in GRP secretion affects tubule formation and in turn angiogenesis, we grew human umbilical vein endothelial cells (HUVECs) using cell culture supernatant from BE(2)-C cells stably-transfected with either shCON or sh*GRPR*. As expected, tubule formation was significantly decreased when HUVECs were grown in media from BE(2)-C cells with sh*GRPR* compared with shCON (**Fig. 1B**). The number of tubules formed by HUVECs grown in media from sh*GRPR* cells was also significantly less in comparison to shCON (2 ± 1 vs 7.3 ± 0.6). To further confirm decreased GRP secretion upon targeted silencing of *GRPR*, neuroblastoma cell lines, BE(2)-C, and BE(2)-M17 were treated with a specific GRPR antagonist, RC-3095. RC-3095 treatment decreased GRP secretion by neuroblastoma cells when compared with DMSO treatment (**Fig. 1C**). We next determined the effects of RC-3095 treatment on HUVEC tubule formation. HUVECs grown in media from BE(2)-C and BE(2)-M17 cells treated with RC-3095 had markedly decreased tubule formation in comparison to DMSO controls (**Fig. 1D**). Taken together, these data show that targeting GRPR decreased GRP secretion by neuroblastoma cells and tubule formation by HUVECs.

Targeting GRPR increased expression of key autophagy proteins

We have previously shown that silencing GRPR inhibits neuroblastoma cell growth and downregulates the PI3K-AKT-RPS6 signaling.[6] Decreased activity of AKT inhibits MTOR signaling and in turn can stimulate autophagy. We investigated the role of GRPR in mediating neuroblastoma cell autophagy. BE(2)-C cells transfected with sh*GRPR* expressed significantly higher levels of ATG12–ATG5 conjugate, ATG16L1, and BECN1 when compared with shCON (**Fig. 2A**). In particular, we observed an increased level of conversion of LC3-I to LC3-II in sh*GRPR* cells (**Fig. 2A**), indicating an activation of the autophagic machinery and formation of autophagosomes. This observation suggests that autophagy is constitutively activated in cells when *GRPR* is silenced. To further visualize the formation of autophagosomes, EGFP-LC3 plasmids were transfected into BE(2)-C/shCON and BE(2)-C/sh*GRPR* cells, and then an autophagy flux assay was performed using the vacuolar H^+-ATPase (V-ATPase) inhibitor bafilomycin A_1 (BafA1) which blocks the fusion of autophagosome with lysosome.[15] Diffuse cytoplasmic localization of EGFP-LC3 was observed in shCON cells, whereas sh*GRPR* cells showed significantly increased punctate fluorescence of LC3 protein at 48 h post-transfection (**Fig. 2B**). In particular, BafA1 increased autophagy flux in sh*GRPR* cells when compared with shCON cells (**Fig. 2B**); these effects of BafA1 were assessed quantitatively by determining the percentage of punctate GFP cells over total GFP transfected cells (**Fig. 2C**). In addition, the expression of SQSTM1/p62, a functional indicator of inhibition of autophagy, was measured. The protein levels of SQSTM1 were dramatically reduced in sh*GRPR* cells in comparison to shCON cells, thus indicating upregulated autophagy (**Fig. 2D**). As expected, BafA1 not only blocked the reduction of SQSTM1 in sh*GRPR* cells, but also significantly increased SQSTM1 expression in shCON cells (**Fig. 2D**).

Using the specific GRPR antagonist, RC-3095, we further confirmed the induction of autophagy in BE(2)-C and BE(2)-M17. RC-3095 treatment increased levels of key autophagy markers like LC3-II, ATG12–ATG5 conjugate, ATG16L1, and BECN1, in comparison to untreated cells (**Fig. 2E**). Moreover, diffuse cytoplasmic localization of EGFP-LC3 was observed in cells without RC-3095 treatment (**Fig. 2F**), which was similar to BE(2)-C/shCON cells (**Fig. 2B**). In contrast, RC-3095 treatment resulted in significantly increased punctate fluorescence of LC3 protein at 48 h post-transfection (**Fig. 2F**), further confirming the observations made in BE(2)-C cells stably transfected to silence *GRPR* (sh*GRPR*) (**Fig. 2B**). In autophagy flux assay, we found that BafA1 significantly increased the punctate fluorescence in RC-3095 treated cells when compared with DMSO-treated cells (**Fig. 2G**). In addition, the levels of SQSTM1 in RC-3095 treated BE(2)-C and BE(2)-M17 cells were decreased (**Fig. 2H**) in a similar fashion to that observed in sh*GRPR* cells (**Fig. 2D**). Moreover, BafA1 treatment alone enhanced SQSTM1 expression in both BE(2)-C and BE(2)-M17 cells, and partially blocked the reduction in SQSTM1 expression after RC-3095 treatment (**Fig. 2H**). These data further confirmed that inhibition of GRPR enhances autophagy in human neuroblastoma cells.

Stimulated autophagy induced autophagosome-mediated degradation of GRP

Autophagy has been implicated in the degradation of peptide and proteins,[16] and appears to negatively regulate angiogenesis by degrading proangiogenic factors.[13] We next sought to determine whether decreased GRP secretion by neuroblastoma cells is due to an increase in autophagy. Rapamycin, a specific inhibitor of MTOR, enhances autophagy.[17,18] We confirmed rapamycin-mediated inhibition of MTOR signaling in BE(2)-C and BE(2)-M17 cell lines, as shown by decreased expression of activated MTOR and RPS6 proteins (**Fig. 3A**). LC3 conversion is a critical step in the process of autophagy and is associated with subsequent degradation of different proteins and organelles within the cell.[16] Rapamycin increased the conversion of LC3-I to LC3-II in both neuroblastoma cell lines examined (**Fig. 3A**).

We then determined the effects of enhanced autophagy on GRP secretion by neuroblastoma cells with the use of rapamycin. BE(2)-C and BE(2)-M17 cell lines were transfected with EGFP-LC3 plasmid and then treated with DMSO or rapamycin for 2 h. Using confocal microscopy, we demonstrated a novel phenomenon where GRP compartmentalizes with the autophagosome marker LC3-II after rapamycin treatment. In contrast to diffuse localization of LC3 in the cytoplasm of DMSO-treated neuroblastoma cells, rapamycin treatment resulted in the formation of typical punctate structures associated with enhanced autophagy (**Fig. 3B**). Interestingly, GRP appeared to be localized within LC3-marked autophagosome in both cell lines (**Fig. 3B**, arrows), indicating that enhanced autophagy induced clearance of GRP in neuroblastoma cells. We also determined that rapamycin treatment significantly decreased GRP secretion in comparison to DMSO-treated

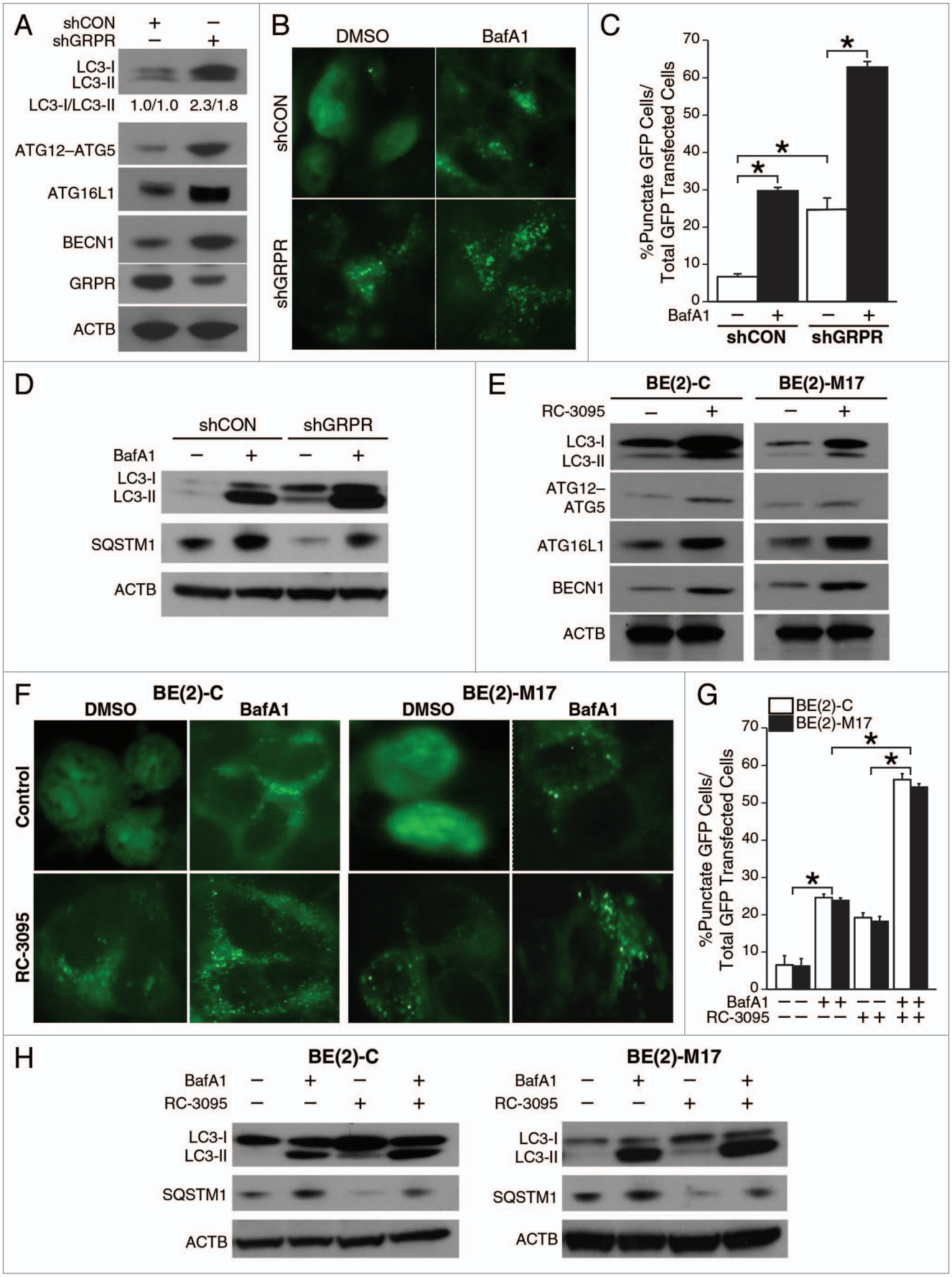

Figure 2 (See opposite page). Inhibition of GRPR enhanced the expression of key autophagic markers in human neuroblastoma cells. (**A**) Immunoblotting demonstrated increased expression of ATG12–ATG5 conjugate, ATG16L1, BECN1 and enhanced conversion of LC3-I to LC3-II in *GRPR*-silenced (sh*GRPR*) BE(2)-C cells when compared with control cells (shCON). (**B**) BE(2)-C cells silenced for *GRPR* (sh*GRPR*) or controls (shCON) were transfected with EGFP-LC3 plasmid and treated with BafA1 (200 μM) for 24 h until assessed for autophagy. Representative fluorescence microscopy photos are shown. (**C**) The percentage of cells with punctate EGFP-LC3 fluorescence was calculated relative to all EGFP-positive cells in BE(2)-C cells (*$P < 0.05$). (**D**) Western blots for LC3-I and -II, and SQSTM1 in BE(2)-C cells silenced for *GRPR* (sh*GRPR*) or control (shCON) and treated with or without BafA1 (200 μM) for 24 h. (**E**) Conversion of LC3-I to LC3-II, ATG12–ATG5 conjugate, ATG16L1, and BECN1 were determined by immunoblotting using lysates from EGFP-LC3-transfected BE(2)-C and BE(2)-M17 cells treated with DMSO or RC-3095 (1 μM) for 48 h. ACTB was probed to assess equal protein loading. (**F**) BE(2)-C and BE(2)-M17 cells were transfected with EGFP-LC3 plasmid, treated with or without BafA1 (200 μM) for 24 h and then assessed for autophagy after 48 h. Representative fluorescence microscopy photos are shown. (**G**) The percentage of cells with punctate EGFP-LC3 fluorescence was calculated relative to all EGFP positive cells in BE(2)-C and BE(2)-M17 cells treated with DMSO or RC-3095 (1 μM). Values shown are mean ± SEM of three separate experiments (*$P < 0.05$). (**H**) Expression of LC3-I or -II, and SQSTM1 in BE(2)-C and BE(2)-M17 cells pretreated with DMSO or RC-3095 (1 μM) and then treated with or without BafA1 (200 μM) for 24 h.

cells (**Fig. 3C**). Together, these results suggest that rapamycin inhibits MTOR signaling, and thereby enhances the formation of autophagosomes leading to increased GRP clearance or degradation by the autophagy-mediated pathway.

Autophagy regulated GRP secretion and angiogenesis via a paracrine mechanism

Since the induction of autophagy inhibited GRP secretion in human neuroblastoma cells, we next wanted to determine the contribution of the proautophagic proteins, ATG5, and BECN1, in this process and subsequently on GRP-mediated angiogenesis in neuroblastoma. We first determined the effects of overexpression of the proautophagic proteins, ATG5, or BECN1, on GRP secretion and tubule formation by HUVECs. Both cell lines, BE(2)-C, and BE(2)-M17, were transfected with plasmids encoding *ATG5* (cDNA *ATG5*), *BECN1* (cDNA *BECN1*), or vector control. Overexpression of ATG5 or BECN1 was confirmed using immunoblotting (**Fig. 4A**). Overexpression of ATG5 or BECN1 increased the production of LC3-II suggesting enhanced autophagy (**Fig. 4A**). As expected, overexpression of proautophagic genes significantly decreased GRP secretion by neuroblastoma cells in comparison to cells transfected with control vector (**Fig. 4B**). To confirm that a decrease in GRP secretion after overexpression of autophagy genes indeed affects angiogenesis we assessed in vitro tubule formation. HUVECs grown in media from ATG5- or BECN1-overexpressing neuroblastoma cells demonstrated reduced tubule formation in vitro when compared with controls (**Fig. 4C**).

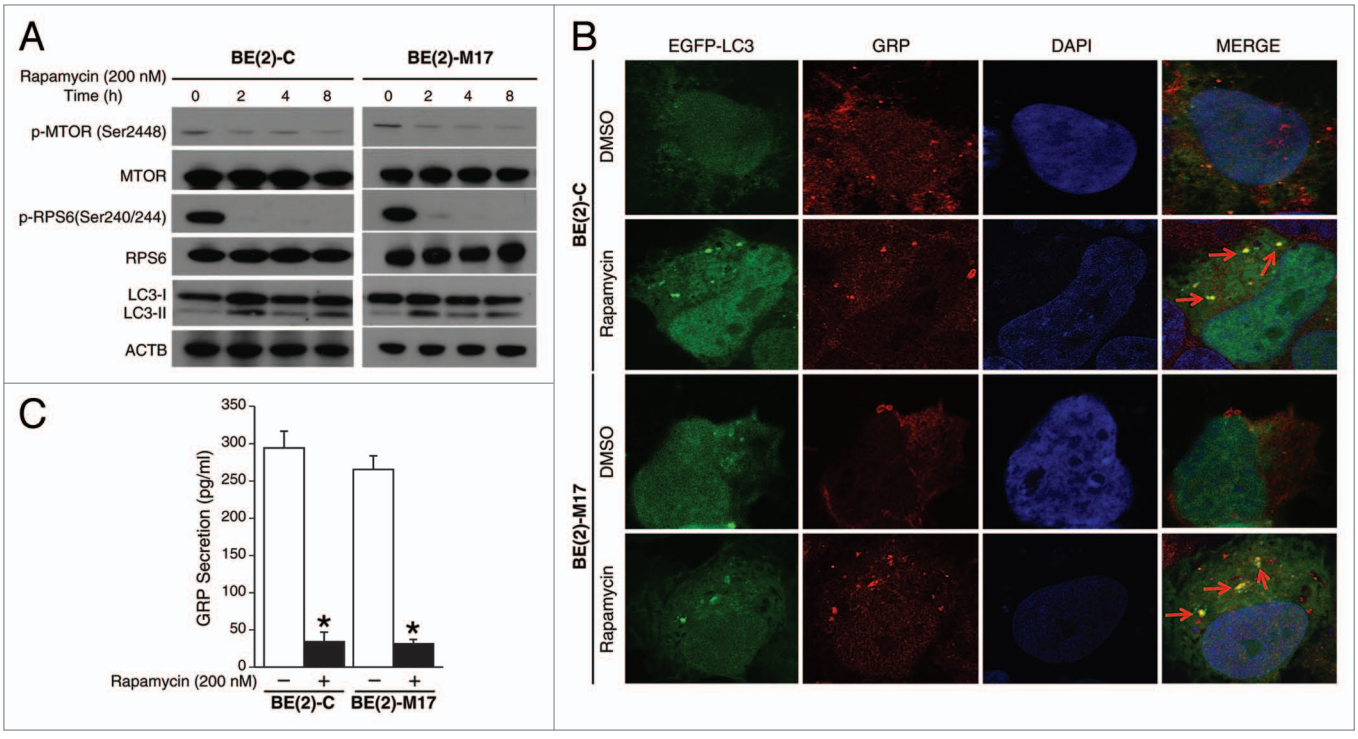

Figure 3. Rapamycin induced co-compartmentalization of GRP and LC3-II. (**A**) BE(2)-C and BE(2)-M17 cells were incubated with rapamycin (200 nM). Total protein was extracted at the indicated time points and probed (35 μg of total protein/lane) with p-MTOR, MTOR, p-RPS6, RPS6, and LC3 antibodies. ACTB was used to monitor equal protein loading. (**B**) BE(2)-C and BE(2)-M17 cells were transfected with an EGFP-LC3 plasmid. At 24 h post-transfection, cells were treated for 2 h with DMSO or rapamycin (200 nM). Cells were fixed and immunostained with antibody against GRP and imaged by confocal microscopy. (**C**) BE(2)-C and BE(2)-M17 cells were plated in serum-free media and treated with DMSO or rapamycin (200 nM) for 48 h. ELISA was used to analyze GRP secretion. Values shown are mean ± SEM of three separate experiments (*$P < 0.05$ vs. no rapamycin).

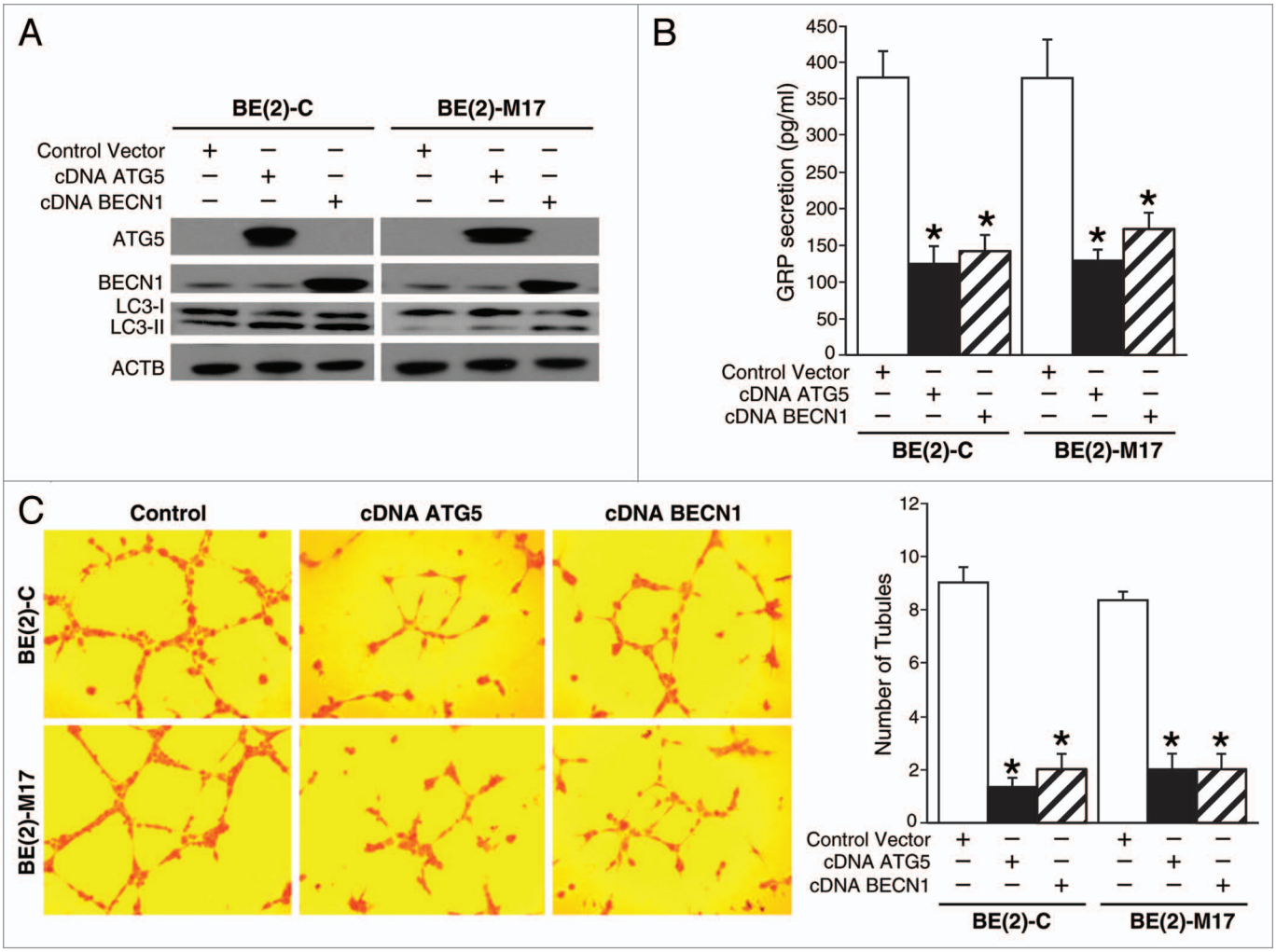

Figure 4. Overexpression of proautophagic molecules decreased GRP secretion and tubule formation by HUVECs. (**A**) ATG5 or BECN1 overexpression and the LC3-II, autophagosome marker, were determined by immunoblotting using lysates from BE(2)-C and BE(2)-M17 cells treated with cDNA encoding ATG5 or BECN1. ACTB was probed to assess equal loading. (**B**) BE(2)-C and BE(2)-M17 cells overexpressing ATG5 or BECN1 were plated on 100 mm dishes in serum-free media for 48 h, and GRP secretion was assessed by ELISA. (**C**) HUVECs were plated on 24-well plates coated with Matrigel and incubated with cell culture media from BE(2)-C or BE(2)-M17 cells overexpressing control vector, cDNA *ATG5* or cDNA *BECN1*. Tubule staining was performed in triplicate and representative images shown. Values shown are mean ± SEM of three separate experiments (*$P < 0.05$ vs. control vector).

Conversely, we determined the effects of silencing key autophagic genes on GRP secretion and in vitro tubule formation by HUVECs. Silencing *ATG5* or *BECN1* using siRNA was confirmed by immunoblotting (**Fig. 5A**). Also, the expression of LC3-II was decreased in cells transfected with either si*ATG5* or si*BECN1*, indicating reduced autophagy (**Fig. 5A**). si*ATG5* or si*BECN1* significantly enhanced GRP secretion by BE(2)-C and BE(2)-M17 cells when compared with cells transfected with nontargeting control (siNTC) (**Fig. 5B**). Furthermore, HUVECs grown in cell culture supernatant from neuroblastoma cells transfected with siRNA against *ATG5* or *BECN1* exhibited increased tubule formation in comparison to controls (**Fig. 5C**). Interestingly, the treatment with a GRP blocking antibody inhibited the increase in tubule formation observed after silencing the autophagic machinery (**Fig. 5C**), thus indicating that this phenomenon is indeed GRP-dependent. Taken together, these data suggest a critical role for autophagy in the regulation of GRP secretion by neuroblastoma cells and tubule formation by HUVECs, indicating a crucial process by which autophagy might modulate GRP-mediated angiogenesis in neuroblastoma.

GRPR inhibition decreased GRP secretion and angiogenesis by activating the autophagic machinery

We next wanted to confirm whether attenuated GRP secretion after GRPR inhibition is indeed autophagy-dependent. Silencing *ATG5* or *BECN1* in sh*GRPR* cells significantly enhanced both GRP secretion (**Fig. 6A**) and tubule formation by HUVECs (**Fig. 6B**) when compared with sh*GRPR* cells transfected with nontargeting control siRNA (siNTC). To further confirm decreased GRP secretion and angiogenesis after targeted inhibition of GRPR, BE(2)-C, and BE(2)-M17 cells were transfected with siRNA against *ATG5*, *BECN1,* or siNTC and then treated with GRPR antagonist, RC-3095. RC-3095-treated cells with either *ATG5* or *BECN1* silencing-agents had

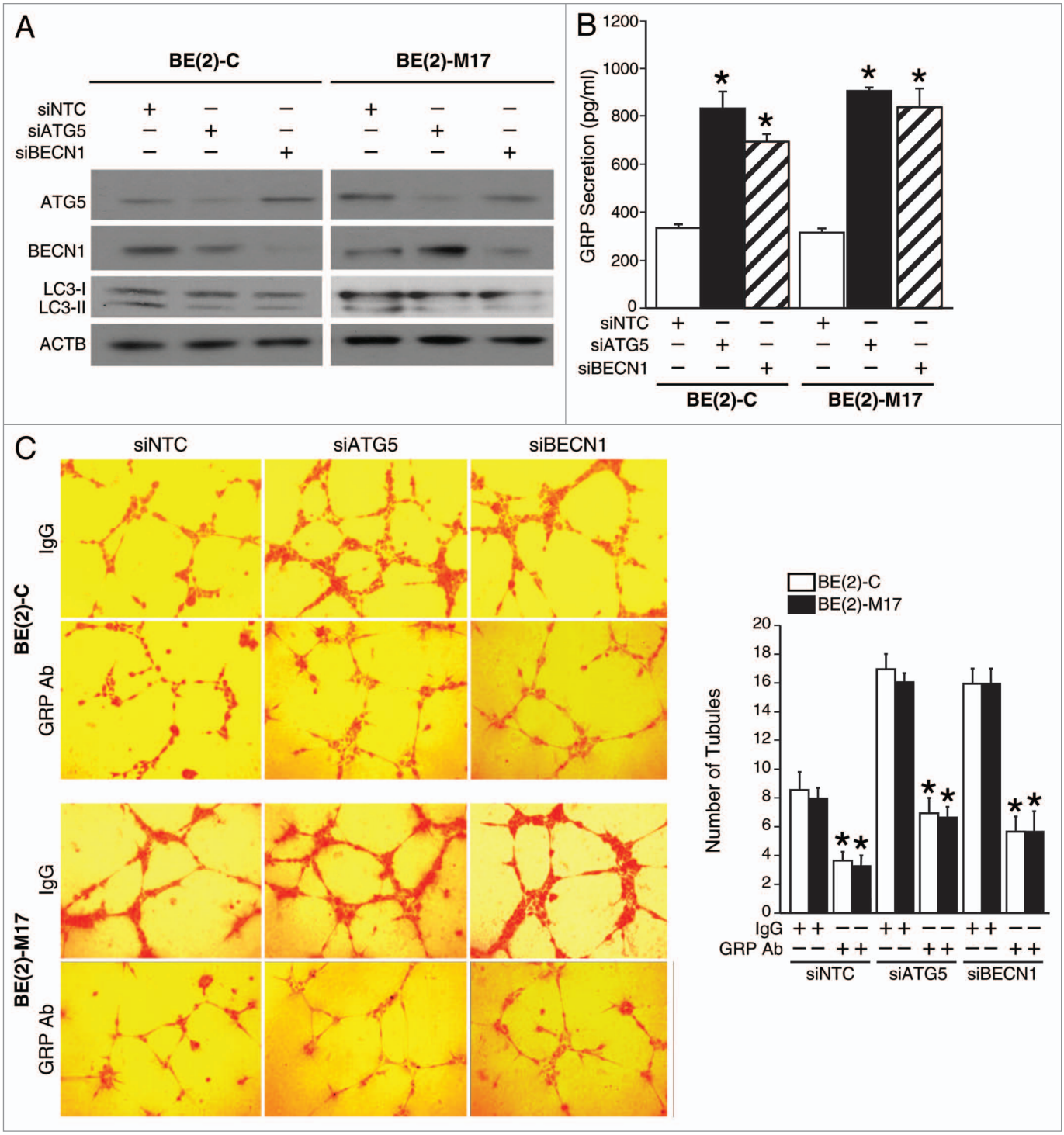

Figure 5. Silencing proautophagic molecules increased GRP secretion and tubule formation by HUVECs. (**A**) *ATG5* or *BECN1* silencing and LC3-II was determined by immunoblotting using lysates from BE(2)-C and BE(2)-M17 cells treated with siRNA against *ATG5* or *BECN1*. ACTB was probed to monitor equal loading. (**B**) BE(2)-C and BE(2)-M17 cells transfected with si*ATG5* or si*BECN1* were plated on 100 mm dishes in serum-free medium for 48 h, and GRP secretion was measured by ELISA. (**C**) HUVECs were plated on 24-well plates coated with Matrigel and incubated with or without GRP antibody (GRP Ab; 1 μg/mL) with cell culture media from BE(2)-C or BE(2)-M17 cells transfected with siNTC, si*ATG5* or si*BECN1*. Tubule staining was performed in triplicate. Values shown are mean ± SEM of three separate experiments (*$P < 0.05$ vs. siNTC or without GRP Ab).

significantly higher GRP secretion in comparison to RC-3095-treated cells transfected with siNTC (**Fig. 6D**). Furthermore, HUVECs grown in media from RC-3095-treated BE(2)-C or BE(2)-M17 cells after *ATG5* or *BECN1* silencing had more tubule formation than RC-3095-treated cells transfected with siNTC (**Fig. 6E**). Taken together, these data confirmed that

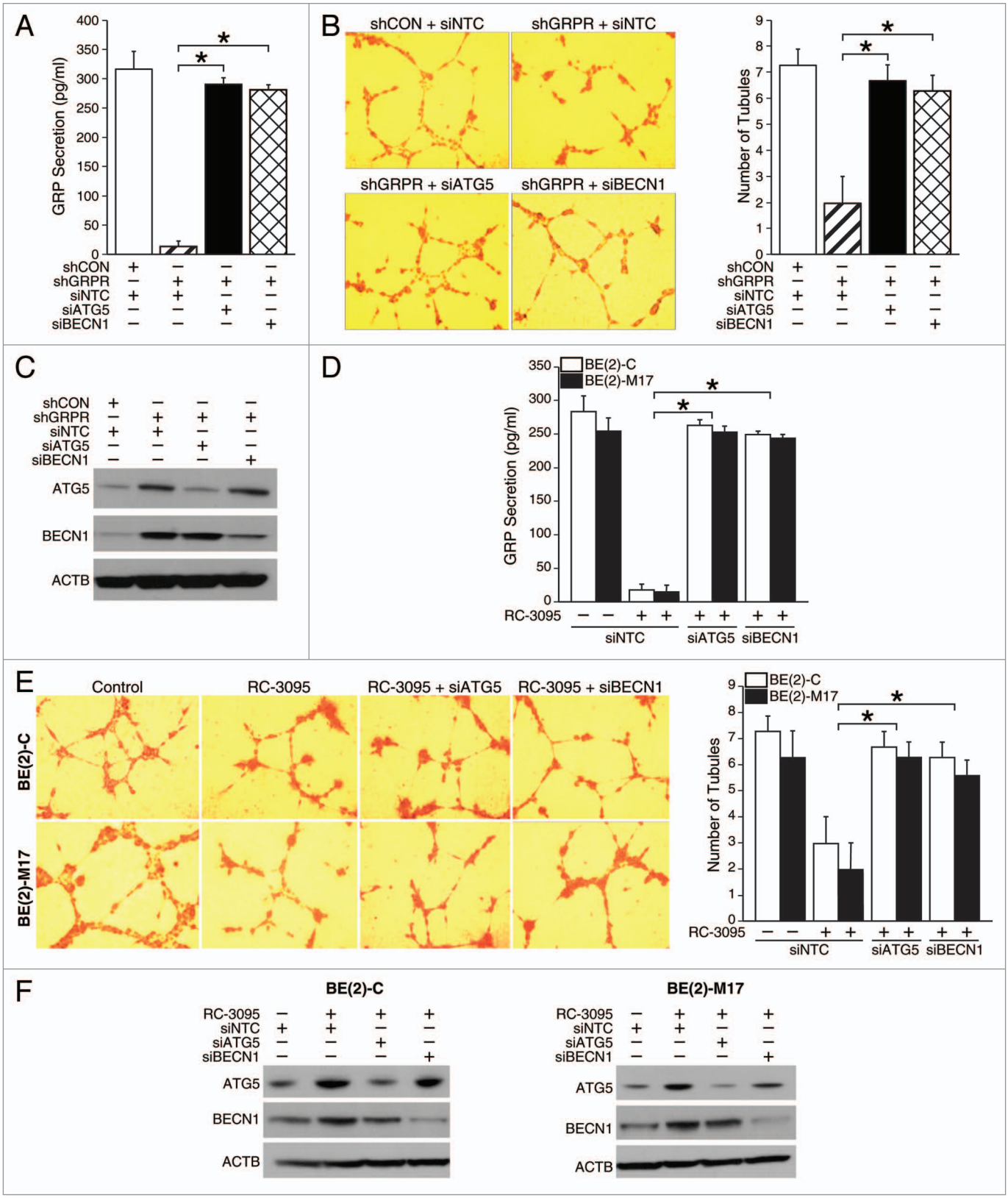

Figure 6. For figure legend, see page 1587.

Figure 6 (See opposite page). Effects of GRP secretion and tubule formation via the autophagy molecules, ATG5 and BECN1, in GRPR-inhibited neuroblastoma cells. (**A**) BE(2)-C/sh*GRPR* cells transfected with si*ATG5* or si*BECN1* were plated in serum-free media for 48 h and analyzed for GRP secretion by ELISA. (**B**) HUVECs were plated on 24-well plates coated with Matrigel and incubated with BE(2)-C cell culture media from sh*GRPR* cells transfected with si*ATG5* or si*BECN1*. Tubules were examined by microscopy and average number of tubules was counted from three separate fields of view. Values shown are mean ± SEM of three separate experiments (*$P < 0.05$). (**C**) *ATG5* and *BECN1* silencing was determined by immunoblotting using lysates from BE(2)-C cells stably-transfected with sh*GRPR* treated with siRNA against *ATG5* or *BECN1*. ACTB was probed to assess equal loading. (**D**) BE(2)-C and BE(2)-M17 cells transfected with si*ATG5* or si*BECN1* were plated in serum-free media and treated with RC-3095 (1 μM) for 48 h. ELISA was used to analyze GRP secretion (*$P < 0.05$). (**E**) HUVECs were plated on 24-well plates coated with Matrigel and incubated with cell culture media from BE(2)-C or BE(2)-M17 cells transfected with si*ATG5* or si*BECN1* treated with RC-3095. Similar to (**B**), tubules were examined by microscopy. Values shown are mean ± SEM of three separate experiments (*$P < 0.05$). (**F**) *ATG5* and *BECN1* silencing was determined by immunoblotting using lysates from BE(2)-C and BE(2)-M17 cells. ACTB was probed to monitor equal loading.

targeting GRPR decreased GRP secretion by neuroblastoma cells and tubule formation by HUVECs due to enhanced autophagy.

Rapamycin-induced autophagy inhibited angiogenesis in vivo

To further confirm that induction of autophagy affected angiogenesis in vivo, we used a xenograft model to induce subcutaneous tumors in the bilateral flank of mice and treated them with either rapamycin or vehicle (saline) daily for 7 d. After sacrifice, tumors were harvested and analyzed. Correlative to in vitro findings (**Fig. 3B**), immunohistochemical analysis of tumor sections from mice treated with rapamycin demonstrated an approximately 4-fold reduction in the number

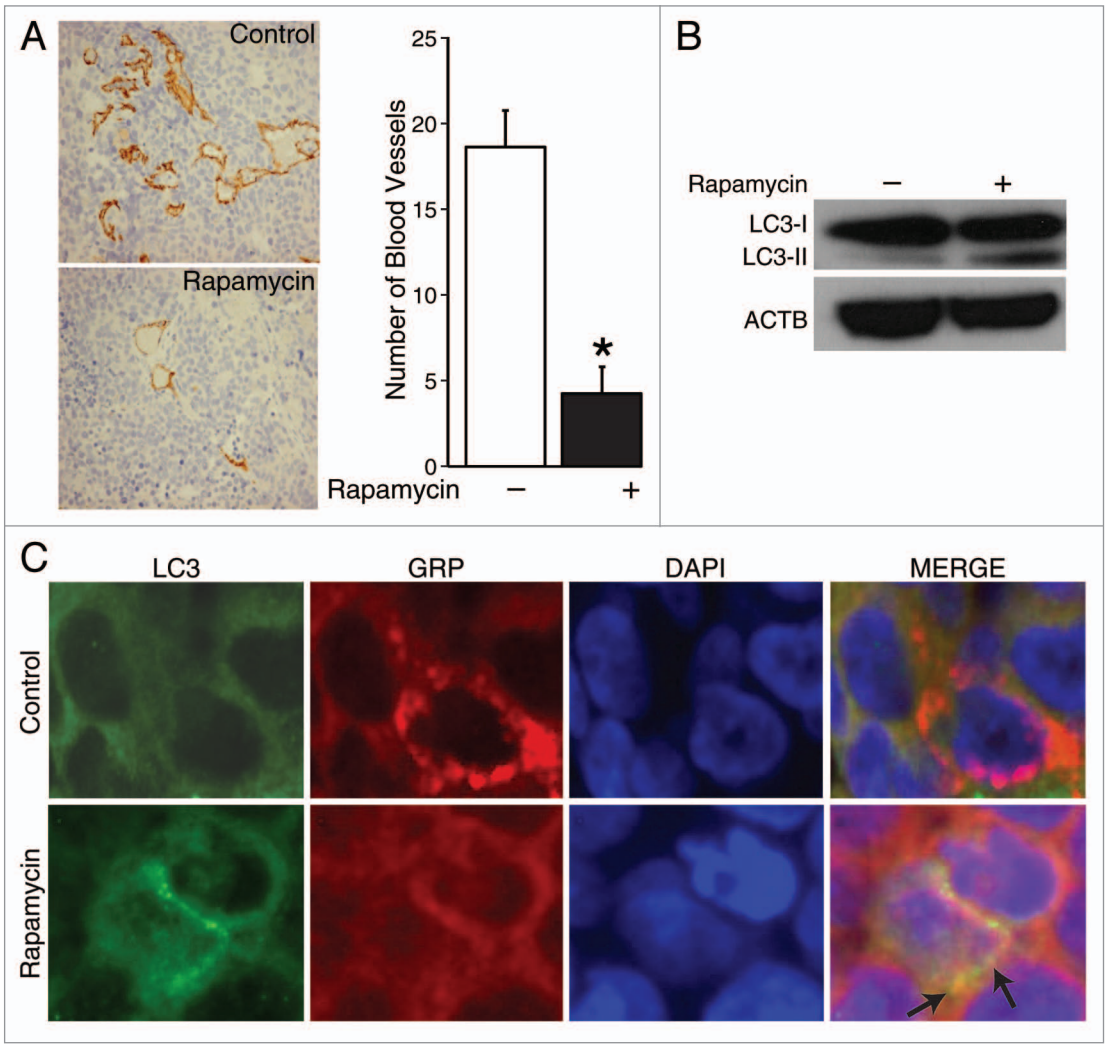

Figure 7. Rapamycin induced co-compartmentalization of GRP and LC3-II in human neuroblastoma xenografts. (**A**) Histological sections were obtained from the tumors harvested from mice in each group and stained for blood vessels using an antibody for PECAM1 (brown stain). Average blood vessel density was determined by counting the number of blood vessels per three randomly selected microscopic fields from multiple xenografts. Values shown are mean ± SEM of three separate experiments (*$P < 0.05$ vs. no rapamycin). (**B**) LC3-I and -II were determined by immunoblots using lysates from three tumors treated with rapamycin or vehicle alone. (**C**) Tissues were fixed and immunostained with antibody against GRP and LC3, and imaged by confocal microscopy.

of PECAM-stained vessels in comparison to tumors from control mice (**Fig. 7A**, brown staining), thus illustrating decreased blood vessel density after rapamycin treatment in vivo. Moreover, the specific action of rapamycin in inducing autophagy in our in vivo model was substantiated by an increased production of LC3-II (**Fig. 7B**). Furthermore, GRP appeared to be localized within LC3-marked autophagosome in tissues (**Fig. 7C**, arrows). Together, these results corroborate our in vitro observations that rapamycin-induced autophagy enhances GRP clearance or degradation by the formation of autophagosomes, which then leads to downregulation of angiogenesis.

Discussion

We have previously reported that GRP, and its receptor, GRPR, are involved in the induction of angiogenesis during neuroblastoma progression.[5] Silencing *GRPR* downregulates the activation of AKT;[6] however, the exact mechanisms of GRPR regulation of MTOR signaling have not yet been elucidated. Targeting MTOR signaling is quite pertinent in neuroblastoma as it negatively regulates autophagy, a cellular process involved in the degradation of long-lived proteins.[16] Recent studies have identified a novel role for autophagy in inhibiting angiogenesis,[11,12] and therefore, we set out to explore whether autophagy might regulate the degradation of GRP, a critical proangiogenic factor in human neuroblastomas.

Here, we describe a novel mechanism where targeted silencing of a cell surface receptor, GRPR, regulated the secretion of its specific ligand, GRP. Since GRP is a critical proangiogenic factor in neuroblastoma angiogenesis, we used an in vitro tubule formation assay to measure the functional significance of decreased GRP secretion by neuroblastoma cells. Decreased GRP secretion exhibited a correlative decrease in tubule formation by vascular endothelial cells. This is consistent with the data that identifies a role for GRP on endothelial cell migration in vitro and angiogenesis in vivo.[19] Moreover, pharmacological inhibition of GRPR using RC-3095 replicated the observations made with the stable GRPR knockdown system. We also demonstrated for the first time that *GRPR* silencing increases the expression of proautophagic proteins and the formation of autophagosomes. RC-3095 treatment converted LC3-I to LC3-II as well as increased EGFP-LC3 puncta, which is a hallmark of autophagy. Moreover, we report that enhanced autophagy increased the degradation of GRP in human neuroblastoma cells. These results suggest a potential application of targeting GRPR to induce autophagy and decrease GRP secretion into the tumor microenvironment, thereby, inhibiting GRP-dependent angiogenesis during neuroblastoma progression. Simultaneous silencing of key autophagic molecules and GRPR increased GRP secretion in comparison to GRPR silencing alone, demonstrating that degradation of GRP after targeting GRPR is indeed due to enhanced autophagy.

Modulation of the autophagic machinery forms a potential tool in targeting tumor growth and angiogenesis.[20-22] Hence, enhancing expression of proautophagic molecules can be used to induce autophagy in neuroblastoma cells, thereby halting their growth and inhibiting tumor cell-mediated angiogenesis. No prior reports exist implicating a role for autophagy in inhibiting angiogenesis in neuroblastoma. Interestingly, our data confirmed this hypothesis as overexpression of ATG5 or BECN1 decreased GRP secretion by neuroblastoma cells and tubule formation by HUVECs. Conversely, si*ATG5* or si*BECN1* enhanced GRP secretion by neuroblastoma cells and increased tubule formation by HUVECs in vitro. Interestingly, blocking GRP using an antibody suppressed the increase in tubule formation observed after silencing the autophagic machinery, indicating a critical role for GRP in neuroblastoma angiogenesis. Moreover, activation of autophagy using inhibitors such as rapamycin might have multiple effects by targeting not only the tumor growth but also tumor-associated neovascularization. This further highlights the complex nature of tumor-stroma interactions and the necessity to target more than one hallmark of cancer for effective anticancer therapies.

In conclusion, we present evidence that autophagy mediates degradation of GRP, which in turn inhibits tumor-associated angiogenesis via a paracrine pathway. To our knowledge, this is the first report of inhibiting GRP-mediated angiogenesis through increased autophagy. Moreover, targeting GRP or GRPR may be potentially used as a novel therapeutic strategy to induce autophagy-mediated neuroblastoma cell death under conditions when apoptosis fails. Autophagy is being progressively regarded as an alternate therapeutic strategy in cancer by targeting multiple hallmarks of cancer. Tumor angiogenesis is related to poor patient outcomes in neuroblastoma patients. Thus, by understanding the relationship between autophagy and its influence on tumor angiogenesis, we may be able to improve overall outcomes for neuroblastoma patients with the aggressive, refractory form of this disease.

Materials and Methods

Cell culture, reagents, and antibodies

Neuroblastoma cells BE(2)-C and BE(2)-M17 were cultured in RPMI 1640 (Mediatech, 10-040-CV) supplemented with 10% fetal bovine serum (Sigma-Aldrich, F2442) at 37 °C and humidified 5% CO_2. HUVECs obtained from Dr M Freeman (Vanderbilt University Medical Center) were cultured in EMM-2 supplemented with Growth Factors (EGM-2 SingleQuot kit, Lonza, CC-4176) at 37 °C and humidified 5% CO_2. BE(2)-C cells were stably transfected with sh*GRPR* or shCON. RC-3095 was purchased from Sigma-Aldrich (R9653). Rapamycin and bafilomycin A_1 were purchased from LC Laboratories (R-5000 and B-1080, respectively). Primary antibodies used include GRPR (Abcam, ab39963), BECN1 (Santa Cruz Biotechnology, sc-11427), LC3 (Novus, NB100-2331), SQSTM1/P62 (Sigma, P0067), and p-MTOR, MTOR, p-RPS6/S6 ribosomal protein, RPS6/S6 Ribosomal, ATG12–ATG5 (Cell Signaling, 2971, 2972, 2215, 2212, and 2630, respectively). GRP blocking antibody was obtained from Tocris Bioscience (1789). PECAM1 polyclonal antibody was purchased from Dianova (DIA310). ACTB/β-actin antibody was from Sigma-Aldrich (A2066).

Endothelial cell tube formation assay

HUVECs grown to ~70% confluence were trypsinized, counted and seeded with various conditioned media at 48,000 cells per well in 24-well plates coated with 300 μl of Matrigel (BD Biosciences, 354234). These cells were periodically observed by microscope as they differentiated into capillary-like tubule structures. After 6 h, cells were stained with H&E and photographs were taken via microscope. The average number of tubules was calculated from examination of three separate microscopic fields (200×) and representative photographs were obtained.

Immunoblotting

Cells (5×10^5) were collected at various time points, and then washed with ice-cold PBS twice before adding lysis buffer (M-PER Mammalian Protein Extraction reagent, Thermo Scientific, 78501), and cocktail inhibitor (Sigma, 5 μg/ml, P8340). Equal amounts of protein were loaded into each well and separated by NuPAGE 4–12% Bis-Tris gel, followed by transfer onto PVDF-membranes (Bio-Rad, 162-0177). Membranes were blocked with 5% nonfat milk in PBS-T for 1 h at room temperature (RT). The blots were then incubated with antibodies against GRPR, p-MTOR, MTOR, p-RPS6, RPS6, ATG12–ATG5 conjugate, BECN1 or LC3, for 1 h at 4 °C. Goat anti-rabbit IgG secondary (1:5000; Santa Cruz Biotechnology, sc-2004) was then incubated for 45 min at RT. Immunoblots were developed by using the chemiluminescence detection system (PerkinElmer, NEL105) and autoradiography was performed. ACTB was used as a loading control.

Autophagy assay

BE(2)-C/shCON, BE(2)-C/sh*GRPR*, BE(2)-C or BE(2)-M17 cells were transfected with 3 μg of EGFP-LC3 expression plasmid (a gift from Dr. Noboru Mizushima) using Lipofectamine 2000 (Invitrogen, 11668) for 24 h. BE(2)-C and BE(2)-M17 cells were treated with RC-3095 (1 μM) for 48 h. The fluorescence of EGFP-LC3 was observed using immunofluorescence microscopy. Cells with punctate GFP signaling were counted as autophagic cells based on characteristic lysosomal localization of LC3 protein during autophagy.[23] Punctate GFP cells were quantified by randomly selecting three separate 100× fields and counting the number of punctate GFP cells per field. The percent of punctate GFP cells per total GFP-transfected cells was calculated and experiments were conducted in triplicate.

GRP secretion assay

The concentration of secreted GRP in cell culture supernatant obtained from neuroblastoma cells was measured using the Enzyme Immunoassay kit (Phoenix Pharmaceuticals, EK-027-07) in accordance with the manufacturer's protocol.

Immunofluorescence staining

Cells were plated on coverslips in 6-well plates and fixed with 3.7% formaldehyde for 10 min at RT. Cells were then permeabilized in 0.2% Triton X-100 for 10 min at RT and were blocked with 1% BSA. After 1 h, the cells were incubated with GRP antibody (1:20) at 4 °C, overnight, followed by an incubation with the secondary antibody (Alexa Fluro 647 goat anti-rabbit, 1:250) at 4 °C for 1 h. The coverslips were mounted with VECTASHIELD mounting medium containing DAPI (Vector Laboratories, H-1200). Images were observed using a confocal microscope (OLYMPUS FV-1000, Cell Imaging Core, Vanderbilt University).

Cell transfection

siRNA against *ATG5*, *BECN1* or nontargeting control (NTC) were purchased from Santa Cruz. Cells were transfected with 25 nM siRNAs using Lipofectamine 2000. Transfected cells were used for subsequent experiments 48 h later. For overexpression, cells were transfected with 3 μg of control vector pcDNA 3.1, pcDNA-*ATG5*, and pcDNA-*BECN1* using Lipofectamine 2000.

In vivo tumor assay

BE(2)-C cells (1×10^6 cells per injection) were subcutaneously injected into scapular regions of athymic nude mice. After 8 d, mice were randomized into either a rapamycin or a control group (n = 5 per group). For rapamycin injections, stock rapamycin was diluted first in sterile 10% PEG400/8% ethanol and then in an equal volume of sterile 10% Tween 80 for a final concentration of 20 μg rapamycin/100 μl. Rapamycin was administered intraperitoneally (i.p.; 2 mg/kg) daily for 7 d. Vehicle was administered i.p. in control mice. After 7 d of treatment, mice were sacrificed and tumors harvested for analyses. Tumors were fixed in formalin and embedded in paraffin, and then prepared in ultra-thin (90 nm) sections. Sections from each treatment group were stained for PECAM1/CD-31 using anti-PECAM1 polyclonal antibody. Average blood vessel density was quantified by randomly selecting three 400× fields and counting the number of blood vessels per field as described previously.[22] GRP and LC3 staining were performed using standard protocols. Images were observed using a confocal microscope (OLYMPUS FV-1000).

Statistical analysis

All results are shown as mean value ± SEM from at least three independent experiments. Immunoblot scans are representative of three independent experiments. Statistical analysis was performed with the the Student *t*-test and P value < 0.05 was considered to be statistically significant.

Disclosure of Potential Conflicts of Interest

No potential conflicts of interest were disclosed.

Acknowledgments

We thank Karen Martin for her assistance with the manuscript preparation. This work was supported by a grant (R01 DK61470) from the National Institutes of Health.

References

1. Brodeur GM. Neuroblastoma: biological insights into a clinical enigma. Nat Rev Cancer 2003; 3:203-16; PMID:12612655; http://dx.doi.org/10.1038/nrc1014
2. Meitar D, Crawford SE, Rademaker AW, Cohn SL. Tumor angiogenesis correlates with metastatic disease, N-myc amplification, and poor outcome in human neuroblastoma. J Clin Oncol 1996; 14:405-14; PMID:8636750
3. Ferrara N, Alitalo K. Clinical applications of angiogenic growth factors and their inhibitors. Nat Med 1999; 5:1359-64; PMID:10581076; http://dx.doi.org/10.1038/70928
4. Kim S, Hu W, Kelly DR, Hellmich MR, Evers BM, Chung DH. Gastrin-releasing peptide is a growth factor for human neuroblastomas. Ann Surg 2002; 235:621-9, discussion 629-30; PMID:11981207; http://dx.doi.org/10.1097/00000658-200205000-00003
5. Kang J, Ishola TA, Baregamian N, Mourot JM, Rychahou PG, Evers BM, Chung DH. Bombesin induces angiogenesis and neuroblastoma growth. Cancer Lett 2007; 253:273-81; PMID:17383815; http://dx.doi.org/10.1016/j.canlet.2007.02.007
6. Qiao J, Kang J, Ishola TA, Rychahou PG, Evers BM, Chung DH. Gastrin-releasing peptide receptor silencing suppresses the tumorigenesis and metastatic potential of neuroblastoma. Proc Natl Acad Sci U S A 2008; 105:12891-6; PMID:18753628; http://dx.doi.org/10.1073/pnas.0711861105
7. Hahn-Windgassen A, Nogueira V, Chen CC, Skeen JE, Sonenberg N, Hay N. Akt activates the mammalian target of rapamycin by regulating cellular ATP level and AMPK activity. J Biol Chem 2005; 280:32081-9; PMID:16027121; http://dx.doi.org/10.1074/jbc.M502876200
8. Kim KW, Mutter RW, Cao C, Albert JM, Freeman M, Hallahan DE, Lu B. Autophagy for cancer therapy through inhibition of pro-apoptotic proteins and mammalian target of rapamycin signaling. J Biol Chem 2006; 281:36883-90; PMID:17005556; http://dx.doi.org/10.1074/jbc.M607094200
9. Kroemer G, Jäättelä M. Lysosomes and autophagy in cell death control. Nat Rev Cancer 2005; 5:886-97; PMID:16239905; http://dx.doi.org/10.1038/nrc1738
10. Glick D, Barth S, Macleod KF. Autophagy: cellular and molecular mechanisms. J Pathol 2010; 221:3-12; PMID:20225336; http://dx.doi.org/10.1002/path.2697
11. Kim JH, Kim JH, Yu YS, Mun JY, Kim KW. Autophagy-induced regression of hyaloid vessels in early ocular development. Autophagy 2010; 6:922-8; PMID:20818164; http://dx.doi.org/10.4161/auto.6.7.13306
12. Lee SJ, Kim HP, Jin Y, Choi AM, Ryter SW. Beclin 1 deficiency is associated with increased hypoxia-induced angiogenesis. Autophagy 2011; 7:829-39; PMID:21685724; http://dx.doi.org/10.4161/auto.7.8.15598
13. Arjamaa O, Nikinmaa M, Salminen A, Kaarniranta K. Regulatory role of HIF-1α in the pathogenesis of age-related macular degeneration (AMD). Ageing Res Rev 2009; 8:349-58; PMID:19589398; http://dx.doi.org/10.1016/j.arr.2009.06.002
14. Cardona C, Bleehen NM, Reeve JG. Characterization of ligand binding and processing by gastrin-releasing peptide receptors in a small-cell lung cancer cell line. Biochem J 1992; 281:115-20; PMID:1310003
15. Yamamoto A, Tagawa Y, Yoshimori T, Moriyama Y, Masaki R, Tashiro Y. Bafilomycin A1 prevents maturation of autophagic vacuoles by inhibiting fusion between autophagosomes and lysosomes in rat hepatoma cell line, H-4-II-E cells. Cell Struct Funct 1998; 23:33-42; PMID:9639028; http://dx.doi.org/10.1247/csf.23.33
16. Eng KE, Panas MD, Karlsson Hedestam GB, McInerney GM. A novel quantitative flow cytometry-based assay for autophagy. Autophagy 2010; 6:634-41; PMID:20458170; http://dx.doi.org/10.4161/auto.6.5.12112
17. Noda T, Ohsumi Y. Tor, a phosphatidylinositol kinase homologue, controls autophagy in yeast. J Biol Chem 1998; 273:3963-6; PMID:9461583; http://dx.doi.org/10.1074/jbc.273.7.3963
18. Blommaart EF, Luiken JJ, Blommaart PJ, van Woerkom GM, Meijer AJ. Phosphorylation of ribosomal protein S6 is inhibitory for autophagy in isolated rat hepatocytes. J Biol Chem 1995; 270:2320-6; PMID:7836465; http://dx.doi.org/10.1074/jbc.270.5.2320
19. Martínez A, Zudaire E, Julián M, Moody TW, Cuttitta F. Gastrin-releasing peptide (GRP) induces angiogenesis and the specific GRP blocker 77427 inhibits tumor growth in vitro and in vivo. Oncogene 2005; 24:4106-13; PMID:15750618; http://dx.doi.org/10.1038/sj.onc.1208581
20. Bae D, Lu S, Taglienti CA, Mercurio AM. Metabolic stress induces the lysosomal degradation of neuropilin-1 but not neuropilin-2. J Biol Chem 2008; 283:28074-80; PMID:18708346; http://dx.doi.org/10.1074/jbc.M804203200
21. Shinohara ET, Cao C, Niermann K, Mu Y, Zeng F, Hallahan DE, Lu B. Enhanced radiation damage of tumor vasculature by mTOR inhibitors. Oncogene 2005; 24:5414-22; PMID:15940265; http://dx.doi.org/10.1038/sj.onc.1208715
22. Kim KW, Hwang M, Moretti L, Jaboin JJ, Cha YI, Lu B. Autophagy upregulation by inhibitors of caspase-3 and mTOR enhances radiotherapy in a mouse model of lung cancer. Autophagy 2008; 4:659-68; PMID:18424912
23. Mizushima N, Yamamoto A, Hatano M, Kobayashi Y, Kabeya Y, Suzuki K, Tokuhisa T, Ohsumi Y, Yoshimori T. Dissection of autophagosome formation using Apg5-deficient mouse embryonic stem cells. J Cell Biol 2001; 152:657-68; PMID:11266458; http://dx.doi.org/10.1083/jcb.152.4.657